

See discussions, stats, and author profiles for this publication at: <https://www.researchgate.net/publication/255001983>

Solvent Effect on the Pore-Size Dependence of an Organic Electrolyte Supercapacitor

ARTICLE *in* JOURNAL OF PHYSICAL CHEMISTRY LETTERS · JULY 2012

Impact Factor: 7.46 · DOI: 10.1021/jz3004624

CITATIONS

62

READS

74

4 AUTHORS, INCLUDING:



Zhehui Jin

Reservoir Engineering Research Institute

18 PUBLICATIONS 333 CITATIONS

SEE PROFILE



Jianzhong Wu

University of California, Riverside

155 PUBLICATIONS 4,323 CITATIONS

SEE PROFILE

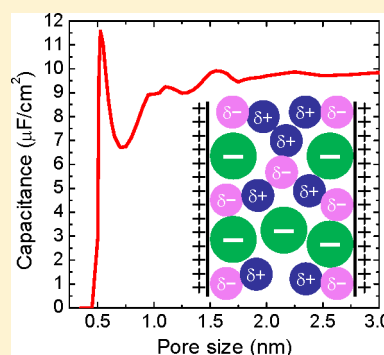
Solvent Effect on the Pore-Size Dependence of an Organic Electrolyte Supercapacitor

De-en Jiang,^{*,†} Zhehui Jin,[‡] Douglas Henderson,[§] and Jianzhong Wu^{*,‡}[†]Chemical Sciences Division, Oak Ridge National Laboratory, Oak Ridge, Tennessee, 37831, United States[‡]Department of Chemical and Environmental Engineering, University of California, Riverside, California 92521, United States[§]Department of Chemistry and Biochemistry, Brigham Young University, Provo, Utah 84602, United States

S Supporting Information

ABSTRACT: Organic electrolytes such as tetraethylammonium tetrafluoroborate dissolved in acetonitrile (TEA-BF₄/ACN) are widely used in commercial supercapacitors and academic research, but conflicting experimental results have been reported regarding the dependence of surface-area-normalized capacitance on the pore size. Here we show from a classical density functional theory the dependence of capacitance on the pore size from 0.5 to 3.0 nm for a model TEA-BF₄/ACN electrolyte. We find that the capacitance–pore size curve becomes roughly flat after the first peak around the ion diameter, and the peak capacitance is not significantly higher than the large-pore average. We attribute the invariance of capacitance with the pore size to the formation of an electric double-layer structure that consists of counterions and highly organized solvent molecules. This work highlights the role of the solvent molecules in modulating the capacitance and reconciles apparently conflicting experimental reports.

SECTION: Energy Conversion and Storage; Energy and Charge Transport



As an attractive technology for electric energy storage, supercapacitors have attracted great interest recently.^{1–8} Also called electrical double-layer capacitors or ultracapacitors, supercapacitors store energy by forming electric double layers of the electrolyte within two symmetric porous carbon electrodes of high surface area and opposite charges. Of great recent interest is the dependence of the surface-area-normalized specific capacitance on the pore size. However, conflicting experimental results have been reported in the case of the popular organic electrolyte, tetraethylammonium tetrafluoroborate (TEA-BF₄) dissolved in acetonitrile (ACN). Chmiola et al. found that the specific capacitance increases greatly when the average pore size of the carbon electrode shrinks to the size of the electrolyte molecules.^{9,10} This so-called “anomalous” increase has been shown for both an ionic-liquid electrolyte¹⁰ and TEA-BF₄/ACN.⁹ However, an experimental study by Centeno et al. on the dependence of the specific capacitance on the pore size for 28 porous carbons showed a “regular” pattern for the TEA-BF₄/ACN electrolyte – the capacitance scatters within ~20% of a constant value of 9.4 μF/cm² for the pore size changing from 0.66 to 15.7 nm.¹¹ This apparent conflict in two experimental studies calls for a theoretical perspective.

In the case of the ionic-liquid electrolyte, the “anomalous” increase in the specific capacitance with the reduction of the pore size has been confirmed by Monte Carlo and molecular dynamics (MD) simulations of different electrode setups (such as slit pores and carbon nanotubes) and electrolyte models (all-atom and coarse-grained) in the small-pore-size range (less than twice the ion diameter).^{12–14} For larger pore sizes and especially up to the mesopore range, a classical density

functional theory predicted that the specific capacitance in fact oscillates with the pore size until it approaches an asymptotic limit when the pore size is beyond eight times the ion diameter.¹⁵ The first cycle of oscillation was also independently observed in two all-atom classical MD simulations,^{16,17} although high computational cost probably prevented simulation of oscillations of capacitance at the larger pore sizes. The long-range oscillations were also confirmed by an analytical theory based on an approximate version of the mean spherical approximation.¹⁸

An intriguing question arises from the oscillatory capacitance of the ionic-liquid electrolyte: whether such a pattern also holds for organic electrolytes such as TEA-BF₄/ACN. This question is highly relevant to the conflicting experimental reports for several reasons: (1) TEA-BF₄/ACN is widely used in commercial supercapacitors and academic studies; (2) theoretical and computational efforts have so far focused on ionic-liquid electrolytes;^{12–16,19–23} (3) the apparent conflict between the “anomalous” increase observed by Chmiola et al.⁹ and the “regular” pattern reported by Centeno et al.¹¹ in the case of TEA-BF₄/ACN should be resolved.

Built on our previous studies of the structure and capacitance of electrolyte/electrode interfaces by using the classical density functional theory,^{24–26} in this Letter we address the question of the role of the polar solvent in the capacitance dependence on

Received: April 17, 2012

Accepted: June 12, 2012

Published: June 12, 2012



the pore size. Like our previous study of the ionic liquid electrolyte,¹⁵ we use a slit-pore model for the porous electrode and the restricted primitive model for the cations and the anions (0.5 nm in diameter); what is new in the present study is that we add solvent molecules to the electrolyte model. Each solvent molecule is represented by a dimer with two hard-sphere segments that have an opposite charge of 0.238 e and a diameter of 0.3 nm, yielding a dipole of 3.4 D comparable to that of ACN.²⁷ We note that very interesting diffusion behavior of the ACN molecule inside the carbon-nanotube electrode has been recently reported.^{28–30} Figure 1 shows a schematic

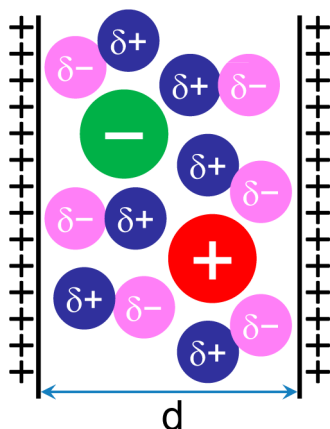


Figure 1. Schematic representation of an organic electrolyte in a porous electrode. Cations and anions are charged hard spheres of 0.5 nm in diameter; the organic solvent is represented by two touching spheres with opposite charge of 0.238 e and the same diameter of 0.3 nm. The electrolyte concentration in the bulk is 1.5 M as used in the experiment.⁹ The pore size is characterized by the width of the slit, d .

representation of our model system; the DFT method to obtain the curve of the surface charge density versus the potential and hence the capacitance for different pore sizes is described in detail in the Supporting Information (SI).

Figure 2 shows the integral capacitance at a surface potential of 1.5 V³¹ as a function of the pore width. (For a smaller

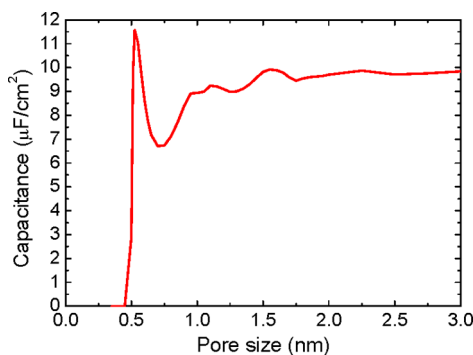


Figure 2. Capacitance of a nanoporous electrode as a function of the pore size for a model system as in Figure 1 at a surface potential of 1.5 V.

voltage at 1.15 V, one can see Figure S1 in the SI, which shows a similar trend). The theoretical prediction displays several interesting features. First, the oscillatory pattern, as shown in the ionic-liquid electrolyte,¹⁵ is all but missing in the model TEA-BF₄/ACN electrolyte. Second, the first peak, as observed in the experiment for the TEA-BF₄/ACN electrolyte as the

“anomalous” increase⁹ is also seen here from the DFT simulation. Third, we observe a slowly varying, nearly constant capacitance beyond 1.0 nm, which is not significantly lower than the first peak. Below we give a detailed analysis of these features.

We first direct our attention to the first peak around 0.5 nm in Figure 2. In the left of the peak, the capacitance quickly decreases to zero due to the size exclusion of the ions inside the slit pore. The right side of the peak shows an increase by 70% in the capacitance as the pore size shrinks from 0.75 to 0.5 nm; the extent of the increase is less than what is reported in the experiment for the TEA-BF₄/ACN electrolyte, where an increase by ~120% was shown.⁹ Here we note that the experimental specific capacitances strongly depend on which method is used to estimate the surface areas of the porous-carbon electrodes for normalization of the capacitances.¹¹ The “anomalous” increase for the pore size approaching the ion diameters has been explained by a phenomenological model^{32,33} and attributed to the desolvation.^{34,35} To test this hypothesis, we plot the average relative densities of the counterion and the solvent as a function of the pore size in Figure 3. As the pore size decreases from 0.75 nm to the ion

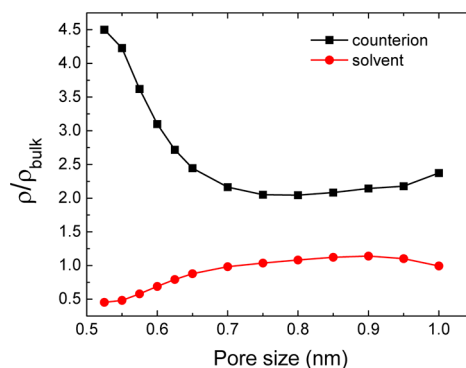


Figure 3. Average relative density (ρ/ρ_{bulk}) of the counterion (anion; black) and the polar solvent (red) inside the pore as a function of the pore width at a surface potential of 1.5 V. ρ_{bulk} is 0.903 nm⁻³ (or 1.5 M) for the ion and 8.49 nm⁻³ (or 14.1 M) for the solvent.

diameter, the average density of the anion increases greatly inside positively charged electrode surfaces, whereas that of the solvent falls. Indeed, desolvation occurs concomitant with the enrichment of the anions as the pore size shrinks to the ion diameter. Figures S2 and S3 in the SI show the density profiles of the ions and the solvent inside the 0.525 and 0.75 nm slit pores, respectively, at the surface potential of 1.5 V. For the 0.525 nm pore where the capacitance peaks, one can see high density of the counterion in a more-or-less single peak, exclusion of the co-ion, and significantly decreased density of the solvent. For the 0.75 nm pore where the capacitance dips, the density of the solvent is recovered, the counterion displays two separate peaks with a reduced height, and the co-ion is still excluded from the slit pore.

From 0.75 to 0.95 nm, the capacitance increases from about 6.7 to 8.9 μF/cm², whereas the average densities of the counterion and the solvent remain roughly flat with the co-ions largely excluded. This indicates that the rise of capacitance from 0.75 nm to 0.95 nm is primarily due to the increase in the total counterion charge with the pore size because for a similar average density a larger pore can accommodate more counterions.

The most interesting feature in Figure 2 is the almost invariance of the capacitance when the pore size is beyond 1.0 nm, distinct from the oscillatory pattern seen in the ionic-liquid electrolyte.¹⁵ To understand this nearly constant capacitance for the model TEA-BF₄/ACN electrolyte, we plot the density profiles of the solvent and the ions inside the pore for different pore sizes. Figure 4 shows the density profiles for the pore size

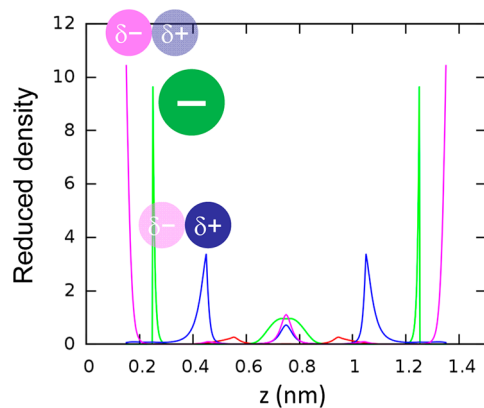


Figure 4. Reduced density profiles of the anion (green), cation (red), the negative segment (pink) of the dipolar solvent, and the positive segment (blue) of the dipolar solvent across the 1.5 nm slit pore at 1.5 V surface potential.

of 1.5 nm at 1.5 V surface potential. One can see that the electric double layers include not only a layer of the counterions (anions in this case) but also a layer of the aligned solvent molecules. Figure 5 shows a schematic depiction of the

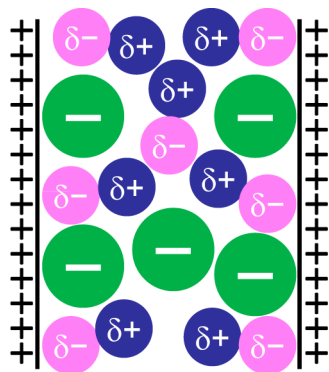


Figure 5. Approximate structure of the ions and the solvent molecules inside the 1.5 nm slit pore with a surface potential of 1.5 V according to the density profiles in Figure 4 but not in proportion.

EDL structure inside the 1.5 nm slit pore. The active participation of the EDL by the polar solvent is a key difference between the ionic-liquid electrolyte and the TEA-BF₄/ACN electrolyte. This conclusion is supported by the fact that the EDL structure at larger pore sizes such as 2.5 nm (Figure 6) is essentially the same as that at 1.5 nm (Figure 4). Therefore, the invariance of the capacitance beyond 1.0 nm pore size shown in Figure 2 can be attributed to the insensitivity of the EDL structure at the electrode surface when it consists of a mixture of counterions and aligned solvent molecules.

Armed with the understanding discussed above, we are now able to reconcile the apparent conflict between the “anomalous” increase⁹ and the “regular” pattern¹¹ for the TEA-BF₄/ACN

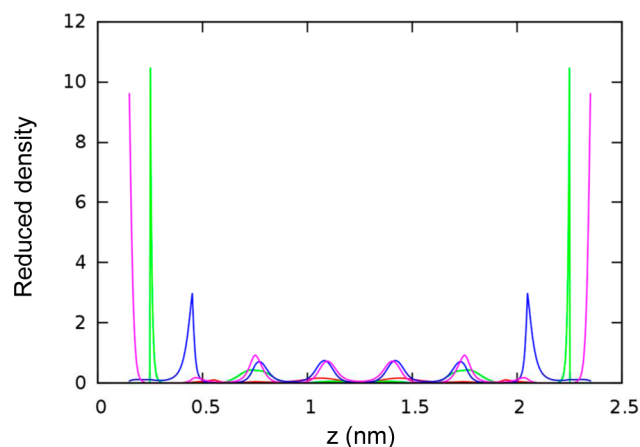


Figure 6. Reduced density profiles of the anion (green), cation (red), the negative segment (pink) of the dipolar solvent, and the positive segment (blue) of the dipolar solvent across the 2.5 nm slit pore at 1.5 V surface potential.

electrolyte in porous carbons. First, Figure 2 does show that the capacitance increases quite a bit as the pore size falls from 0.75 to 0.5 nm (the ion diameter), vindicating the “anomalous” increase; second, we also see a roughly flat capacitance beyond 1.0 nm pore size, in agreement with the “regular” pattern. The key question is whether the “anomalous” increase or the capacitance at the first peak is significant in comparison with the average value at the large pore size. Our DFT results show that the peak capacitance (at ~ 0.5 nm) is $\sim 17\%$ higher than the average capacitance between 1.0 and 3.0 nm for the 1.5-V surface potential (and 13% higher for the 1.15-V surface potential; see Figure S1 in the SI). This amount of increase is probably not significant, given the measured values for 28 porous carbons of different pore sizes scattering within $\sim 20\%$ of the constant value in the “regular” pattern.¹¹ In addition, the “anomalous” increase happens within a very narrow pore-size range of 0.75 to 0.5 nm (the ion diameter). To observe the increase distinctively, one needs to control the pore size precisely and the pore-size distribution to be as narrow as possible. Any dispersion in the pore size distribution or slight breathing of the pore structure³⁶ during charging/discharging is likely to compromise the modest capacitance increases. Very recently, the effect of pore size distribution on the capacitance has been discussed for the case of an ionic liquid electrolyte.²⁰

We may also make a quantitative comparison of the capacitance values between the present DFT results and the experiment for the large-pore limit. As shown in Figure 2, the DFT yields an average value of $9.8 \mu\text{F}/\text{cm}^2$, whereas Centeno et al.’s experiment gave an average of $9.4 \mu\text{F}/\text{cm}^2$. Given the extremely simplified model we used for the TEA-BF₄/ACN system, the agreement between the experiment and our DFT results is truly remarkable. The DFT value also agrees well with the capacitance derived from an all-atom classical MD simulation of the TEA-BF₄/ACN electrolyte inside a slit pore with a large separation (3.9 nm).³⁷

In summary, we have provided a new perspective into the dependence of the surface-area-normalized capacitance on the pore size of a model organic electrolyte (tetraethylammonium tetrafluoroborate dissolved in acetonitrile) inside nanopores of a supercapacitor. The theoretical goal was two-fold: to contrast with the ionic-liquid electrolyte and to reconcile previous conflicting experimental reports. Unlike the ionic liquid

electrolyte where the specific capacitance strongly oscillates with variation of the pore size, in the case of the organic electrolyte the capacitance is relatively insensitive to the pore size beyond the first peak, in agreement with the “regular” pattern.¹¹ In comparison with the capacitance minimum near 0.75 nm pore size (or 1.5 times the ion diameter), the first peak corresponds to the “anomalous” increase,⁹ but the degree of enhancement is much less than the previous experiment suggested, and the peak value is only ~17% higher than the capacitance in the large-pore limit. The relatively constant capacitance beyond twice the ion diameter is due to the formation of an EDL at the electrode that consists of both counterions and highly organized solvent molecules. This work offers a reconciliatory picture of the capacitance dependence on the pore size and suggests an important role for the polar solvent to participate in the EDL formation.

■ ASSOCIATED CONTENT

■ Supporting Information

Details of the density functional theory method employed, capacitance at the 1.15 V surface potential, and density profiles inside the 0.525 and 0.75 nm slit pores. This material is available free of charge via the Internet at <http://pubs.acs.org/>.

■ AUTHOR INFORMATION

Corresponding Author

*E-mail: jiangd@ornl.gov (D.J.); jwu@engr.ucr.edu (J.W.).

Notes

The authors declare no competing financial interest.

■ ACKNOWLEDGMENTS

D.J. was supported as part of the Fluid Interface Reactions, Structures, and Transport (FIRST) Center, an Energy Frontier Research Center funded by the U.S. Department of Energy, Office of Science, Office of Basic Energy Sciences. Additional support (J.W.) is provided by the National Science Foundation (NSF-CBET-0852353). This research also used resources of the National Energy Research Scientific Computing Center (NERSC), which is supported by the Office of Science of the U.S. Department of Energy under contract no. DE-AC02-05CH11231.

■ REFERENCES

- (1) Miller, J. R.; Simon, P. Electrochemical Capacitors for Energy Management. *Science* **2008**, *321*, 651–652.
- (2) Simon, P.; Gogotsi, Y. Materials for Electrochemical Capacitors. *Nat. Mater.* **2008**, *7*, 845–854.
- (3) Futaba, D. N.; Hata, K.; Yamada, T.; Hiraoka, T.; Hayamizu, Y.; Kakudate, Y.; Tanaike, O.; Hatori, H.; Yumura, M.; Iijima, S. Shape-Engineerable and Highly Densely Packed Single-Walled Carbon Nanotubes and Their Application as Supercapacitor Electrodes. *Nat. Mater.* **2006**, *5*, 987–994.
- (4) Chmiola, J.; Largeot, C.; Taberna, P. L.; Simon, P.; Gogotsi, Y. Monolithic Carbide-Derived Carbon Films for Micro-Supercapacitors. *Science* **2010**, *328*, 480–483.
- (5) Miller, J. R.; Outlaw, R. A.; Holloway, B. C. Graphene Double-Layer Capacitor with ac Line-Filtering Performance. *Science* **2010**, *329*, 1637–1639.
- (6) Zhu, Y. W.; Murali, S.; Stoller, M. D.; Ganesh, K. J.; Cai, W. W.; Ferreira, P. J.; Pirkle, A.; Wallace, R. M.; Cychoz, K. A.; Thommes, M.; et al. Carbon-Based Supercapacitors Produced by Activation of Graphene. *Science* **2011**, *332*, 1537–1541.
- (7) Izadi-Najafabadi, A.; Yamada, T.; Futaba, D. N.; Yudasaka, M.; Takagi, H.; Hatori, H.; Iijima, S.; Hata, K. High-Power Supercapacitor Electrodes from Single-Walled Carbon Nanohorn/Nanotube Composite. *ACS Nano* **2011**, *5*, 811–819.
- (8) El-Kady, M. F.; Strong, V.; Dubin, S.; Kaner, R. B. Laser Scribing of High-Performance and Flexible Graphene-Based Electrochemical Capacitors. *Science* **2012**, *335*, 1326–1330.
- (9) Chmiola, J.; Yushin, G.; Gogotsi, Y.; Portet, C.; Simon, P.; Taberna, P. L. Anomalous Increase in Carbon Capacitance at Pore Sizes Less than 1 Nanometer. *Science* **2006**, *313*, 1760–1763.
- (10) Largeot, C.; Portet, C.; Chmiola, J.; Taberna, P. L.; Gogotsi, Y.; Simon, P. Relation between the Ion Size and Pore Size for an Electric Double-Layer Capacitor. *J. Am. Chem. Soc.* **2008**, *130*, 2730–2731.
- (11) Centeno, T. A.; Sereda, O.; Stoeckli, F. Capacitance in Carbon Pores of 0.7 to 15 nm: A Regular Pattern. *Phys. Chem. Chem. Phys.* **2011**, *13*, 12403–12406.
- (12) Yang, L.; Fishbine, B. H.; Migliori, A.; Pratt, L. R. Molecular Simulation of Electric Double-Layer Capacitors Based on Carbon Nanotube Forests. *J. Am. Chem. Soc.* **2009**, *131*, 12373–12376.
- (13) Shim, Y.; Kim, H. J. Nanoporous Carbon Supercapacitors in an Ionic Liquid: A Computer Simulation Study. *ACS Nano* **2010**, *4*, 2345–2355.
- (14) Kondrat, S.; Georgi, N.; Fedorov, M. V.; Kornyshev, A. A. A Superionic State in Nano-Porous Double-Layer Capacitors: Insights from Monte Carlo Simulations. *Phys. Chem. Chem. Phys.* **2011**, *13*, 11359–11366.
- (15) Jiang, D. E.; Jin, Z. H.; Wu, J. Z. Oscillation of Capacitance inside Nanopores. *Nano Lett.* **2011**, *11*, 5373–5377.
- (16) Wu, P.; Huang, J.; Meunier, V.; Sumpter, B. G.; Qiao, R. Complex Capacitance Scaling in Ionic Liquids-Filled Nanopores. *ACS Nano* **2011**, *5*, 9044–9051.
- (17) Feng, G.; Cummings, P. T. Supercapacitor Capacitance Exhibits Oscillatory Behavior as a Function of Nanopore Size. *J. Phys. Chem. Lett.* **2011**, *2*, 2859–2864.
- (18) Henderson, D. Oscillations in the Capacitance of a Nanopore Containing an Electrolyte due to Pore Width and Nonzero Size Ions. *J. Colloid Interface Sci.* **2012**, *374*, 345–347.
- (19) Merlet, C.; Rotenberg, B.; Madden, P. A.; Taberna, P.-L.; Simon, P.; Gogotsi, Y.; Salanne, M. On the Molecular Origin of Supercapacitance in Nanoporous Carbon Electrodes. *Nat. Mater.* **2012**, *11*, 306–310.
- (20) Kondrat, S.; Perez, C. R.; Presser, V.; Gogotsi, Y.; Kornyshev, A. A. Effect of Pore Size and its Dispersity on the Energy Storage in Nanoporous Supercapacitors. *Energy Environ. Sci.* **2012**, *5*, 6474–6479.
- (21) Vatamanu, J.; Borodin, O.; Smith, G. D. Molecular Insights into the Potential and Temperature Dependences of the Differential Capacitance of a Room-Temperature Ionic Liquid at Graphite Electrodes. *J. Am. Chem. Soc.* **2010**, *132*, 14825–14833.
- (22) Vatamanu, J.; Borodin, O.; Smith, G. D. Molecular Simulations of the Electric Double Layer Structure, Differential Capacitance, and Charging Kinetics for *N*-Methyl-*N*-propylpyrrolidinium Bis-(fluorosulfonyl)imide at Graphite Electrodes. *J. Phys. Chem. B* **2011**, *115*, 3073–3084.
- (23) Rajput, N. N.; Monk, J.; Singh, R.; Hung, F. R. On the Influence of Pore Size and Pore Loading on Structural and Dynamical Heterogeneities of an Ionic Liquid Confined in a Slit Nanopore. *J. Phys. Chem. C* **2012**, *116*, 5169–5181.
- (24) Jiang, D. E.; Meng, D.; Wu, J. Z. Density Functional Theory for Differential Capacitance of Planar Electric Double Layers in Ionic Liquids. *Chem. Phys. Lett.* **2011**, *504*, 153–158.
- (25) Wu, J. Z.; Jiang, T.; Jiang, D. E.; Jin, Z. H.; Henderson, D. A Classical Density Functional Theory for Interfacial Layering of Ionic Liquids. *Soft Matter* **2011**, *7*, 11222–11231.
- (26) Henderson, D.; Wu, J. Z. Electrochemical Properties of the Double Layer of an Ionic Liquid Using a Dimer Model Electrolyte and Density Functional Theory. *J. Phys. Chem. B* **2012**, *116*, 2520–2525.
- (27) Partington, J. R.; Cowley, E. G. Dipole Moment of Acetonitrile. *Nature* **1935**, *135*, 474–474.
- (28) Kalugin, O. N.; Chaban, V. V.; Loskutov, V. V.; Prezhdov, O. V. Uniform Diffusion of Acetonitrile inside Carbon Nanotubes Favors Supercapacitor Performance. *Nano Lett.* **2008**, *8*, 2126–2130.

(29) Chaban, V. Filling Carbon Nanotubes with Liquid Acetonitrile. *Chem. Phys. Lett.* **2010**, *496*, 50–55.

(30) Izadi-Najafabadi, A.; Futaba, D. N.; Iijima, S.; Hata, K. Ion Diffusion and Electrochemical Capacitance in Aligned and Packed Single-Walled Carbon Nanotubes. *J. Am. Chem. Soc.* **2010**, *132*, 18017–18019.

(31) The integral capacitance is defined as $C = Q/(\varphi_0 - \psi_{PZC})$, where Q is the surface charge density, φ_0 is electrode surface potential, and ψ_{PZC} is the potential at the point of zero charge. We chose $\varphi_0 - \psi_{PZC} = 1.5$ V to obtain the integral capacitance, and ψ_{PZC} is zero in the case of the symmetric dimer model shown in Figure 1. See the Supporting Information for a detailed explanation.

(32) Huang, J. S.; Sumpter, B. G.; Meunier, V. Theoretical Model for Nanoporous Carbon Supercapacitors. *Angew. Chem., Int. Ed.* **2008**, *47*, 520–524.

(33) Huang, J. S.; Sumpter, B. G.; Meunier, V. A Universal Model for Nanoporous Carbon Supercapacitors Applicable to Diverse Pore Regimes, Carbon Materials, and Electrolytes. *Chem.—Eur. J.* **2008**, *14*, 6614–6626.

(34) Chmiola, J.; Largeot, C.; Taberna, P. L.; Simon, P.; Gogotsi, Y. Desolvation of Ions in Subnanometer Pores and its Effect on Capacitance and Double-Layer Theory. *Angew. Chem., Int. Ed.* **2008**, *47*, 3392–3395.

(35) Simon, P.; Gogotsi, Y. Charge Storage Mechanism in Nanoporous Carbons and its Consequence for Electrical Double Layer Capacitors. *Philos. Trans. R. Soc., A* **2010**, *368*, 3457–3467.

(36) Hantel, M. M.; Presser, V.; Kötz, R.; Gogotsi, Y. In situ Electrochemical Dilatometry of Carbide-derived Carbons. *Electrochem. Commun.* **2011**, *13*, 1221–1224.

(37) Feng, G.; Huang, J.; Sumpter, B. G.; Meunier, V.; Qiao, R. Structure and Dynamics of Electrical Double Layers in Organic Electrolytes. *Phys. Chem. Chem. Phys.* **2010**, *12*, 5468–5479.